

**MISTI 31.15.03.**

## **AEROSOL METHOD FOR OBTAINING THIN FILMS OF DOPED BISMUTH VANADATE FOR WATER PHOTOLYSIS**

**Seitmagzimov A.A.<sup>1</sup>, Seitmagzimova G.M.<sup>1\*</sup>, Seitmagzimova L.A.<sup>2</sup>**

<sup>1</sup>*M.Auezov South Kazakhstan University, Shymkent, Kazakhstan*

<sup>2</sup>*JSC "KAZNIICHEMPROJECT", Shymkent, Kazakhstan*

**\*Corresponding author's e-mail:** galinaseit@mail.ru

### **ABSTRACT**

The article presents the results of research of obtaining bismuth vanadate films for processes of water photolysis by simple and reliable method of aerosol spraying of water solutions. Films of bismuth vanadate doped with molybdenum were obtained on the surface of conducting glasses. For hydrogen production systems, this is a compact, inexpensive and fast method/ At that photocurrents at a level of 1.5 mA to silver chloride reference electrode were obtained in the phosphate electrolyte with an external bias of 1.5 V, and up to 3.5 mA with addition of sulfite electrolyte. It is shown that molybdenum addition leads to an insignificant expansion and enhancement of the band in the region of 350-550 nm, and in general the system spectral characteristics are insignificant, while the system current characteristics increase significantly, 6-7 times. This is explained by increase in the mobility of electrons and holes, or by increased concentration of charge carriers caused by electron-donor elements, in particular, molybdenum. On the other hand, we associate this with the hypothesis that Mo (VI) replaces V (V) in the monoclinic main lattice of BiVO<sub>4</sub> of scheelite type [23]; i.e. inclusion of Mo into BiVO<sub>4</sub> leads to the stabilization of the tetragonal scheelite type in solid solutions in rather narrow range of compositions, which leads to a significant decrease in the current load in the system.

**Keywords:** photocurrent, molybdenum, bismuth vanadate, alloying, sacrificial electrolyte, flat zone potential.

### **INTRODUCTION**

Bismuth vanadate (BiVO<sub>4</sub>) is considered as one of the most promising photocatalysts for water photolysis and is of increasing interest as a model photoanode for oxygen evolution [1–10], which has an inherent (indirect) band gap of 2.4–2.5 eV (496–517 nm), optical absorption coefficient equal to 10<sup>4</sup>-10<sup>5</sup> cm<sup>-1</sup> for  $h\nu = 2.5\text{--}3.5$  and the potential of flat bands 200 mV to the left of hydrogen evolution reaction (HER). This characterizes such parameters of an electrochemical cell as maximum theoretical photocurrent equal to 6.2-7.5 mA/cm<sup>2</sup> and the efficiency of converting solar energy into hydrogen, equal to 7.6–9.2% paired with an ideal photocathode [11] in a tandem water separating device [11-14]. But disadvantages are also inherent for it, such as suboptimal band gap and poor charge transfer through a sample array due to the high rate of carrier recombination. Bismuth vanadate is characterized by short diffusion of charge carriers, which characterizes diffusion lengths of only 70 nm, which is the main reason for low photocurrent density, namely less than 1 mA/cm<sup>2</sup> at potentials close to

1.23 V to reversible hydrogen electrode ratio [15-18]. Other disadvantages of bismuth vanadate include its weak activity in relation to the hydrogen evolution in catalyst absence [19], as well as low corrosion stability, especially in aggressive acidic environments (pH below 3) or alkaline ones (pH above 11) [20]. This is naturally undesirable to avoid ionic gradients and mass transfer limitations in practical solar fuel generators [21-23]. The aim of this work is to study the doping effect of molybdenum ions on bismuth vanadate and characteristics of bismuth vanadate-molybdenum system, such as spectral, current, and morphological ones when using the aerosol method of coating on various substrates.

## **MATERIALS AND METHODS**

For the research, reagents of "pure" or "chemically pure" qualifications were used, namely bismuth nitrate  $\text{Bi}(\text{NO}_3)_3 \cdot 5\text{H}_2\text{O}$ , corresponding to GOST 4110-75, and ammonium vanadate  $\text{NH}_4\text{VO}_3$ , corresponding to GOST 9336-75, as well as concentrated nitric acid, acetone and alcohol. To obtain coatings on conducting glass, LATECH FTO glasses (conductivity less than  $15 \text{ ohm/cm}^2$ ) with a size of  $1 \times 2.5 \text{ cm}^2$  were used, which were degreased in soda ash solution and ultrasound, sequentially washed in isopropanol, acetone, and dried.

To obtain films of bismuth vanadate, the following procedure was used: 2 ml of 0.2% ammonium vanadate water solution (No.1 solution) was acidified with nitric acid. Then 3 ml of 1.2% bismuth nitrate solution (No.2 solution) was added to it. The resulting mixture was applied with a spray gun onto prepared glass, preheated to a temperature of  $100\text{-}120^\circ\text{C}$ . A conventional (household) spray bottle for aerosol water mixtures was used as a spray bottle. 10, 20 and 30 cycles of applying such a mixture to glass and metallic platinum was used, after which the samples were dried at  $60^\circ\text{C}$  for 1 hour, then annealed in a muffle furnace at  $500^\circ\text{C}$  for 1 hour. For alloying, 10, 20, 30 and 40 mg of a weighed portion of ammonium molybdate was added to 2 ml of No.2 solution, and then 3 ml of No.1 solution was added. Obtained solutions contained 0.2, 0.4, 0.6 and 0.8%  $(\text{NH}_4)_2\text{MoO}_4$ , respectively. Subsequently, the deposition of coatings was carried out in the same way like for initial bismuth vanadate.

Anodic photocurrents of titanium oxide electrodes were recorded according to a three-electrode scheme; a platinum wire was used as a counter electrode; silver chloride reference electrode was used. A xenon lamp without light filters was used to illuminate iron oxide films. Illumination of the samples was measured with a lux meter and was  $(160\text{-}180) \cdot 10^3 \text{ lux}$  for a xenon lamp and  $12 \cdot 10^3 \text{ lux}$  for a UV lamp. The illumination level in the sun at the latitude of Shymkent in June, measured at noon, was  $130 \cdot 10^3 \text{ lux}$ .

For photoelectrochemical studies, two types of electrolytes were used: a neutral one as 0.1M  $\text{KH}_2\text{PO}_4$  solution, as well as a complex electrolyte as 0.1M  $\text{KH}_2\text{PO}_4$  solution with 0.5M  $\text{Na}_2\text{SO}_3$  solution addition in the form of a so-called "sacrificial" solution. It is called that in the literature, "as a sacrificial reagent".

Microphotographs of the film were taken with the use of JSM-6490LV scanning electron microscope (JEOL, Japan). Absorption spectra on glass were obtained using a Cary-50 UV-visible spectrophotometer.

## **RESULTS AND DISCUSSION**

Fig. 1 shows the absorption spectra of bismuth vanadate obtained on glass after calcination at a temperature of  $500^\circ\text{C}$  (line 2) and bismuth vanadate doped with molybdenum (line 1).

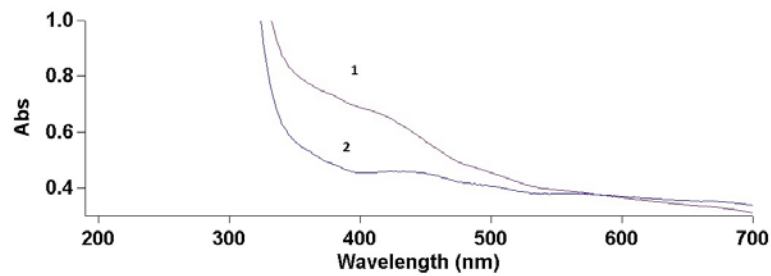


Fig 1. Absorption spectra of bismuth vanadate (2), and bismuth vanadate doped with molybdenum (1)

If to estimate the band gap of the sample (2) according to the equation [25], as  $E_g(\text{eV})=1240/\lambda$ , where  $\lambda$  is the wavelength, then you can see two half-waves: a small one in the region of 400 nm, which corresponds to 3.1 eV and the second wave at 500 nm, which corresponds to 2.48 eV. The absorption spectra in the ultraviolet-visible region, obtained for films deposited on a glass slide support, are in the range of 400-500 nm, i.e. it is a part of the visible spectral range, which is in good agreement with the data of [26].

The band gap of thin films of bismuth vanadate was calculated using the Kubelka – Munk formula [26]. The obtained value of  $E_g$  is 2.55 eV and agrees with theoretical predictions (2.60 eV) made for a partially reconstructed cluster ( $\text{BiVO}_4$ ) with a size of 1.2 nm. One can see the expansion of the absorption band (350-500 nm), which is associated with the appearance of molybdenum in the film composition (line 1). At the same time, the publication [27] did not reveal changes in the spectra of samples with a content of 3% molybdenum, while in publication [28] on samples with a content of 1-1.8% molybdenum, there is a slight absorption in the region of 350-500 nm. Absorption was similarly found in the authors' reference [29]. In our case, we see that doping with molybdenum leads to the broadening and strengthening of the band in the 350-550 nm region.

As for chemical composition of the film, it can be seen on the spectrogram (Figure 2) that molybdenum is present in the film composition up to 6%, and this is reflected in the spectral part of the films in Figure 1. It should be assumed that true elemental chemical composition of the film on molybdenum differs from that shown in Figure 2, because it shows the local change in the molybdenum content in the film composition. We did not analyze the true value of molybdenum on the glass surface. This requires a more accurate measurement of molybdenum content in the film composition in the glass.

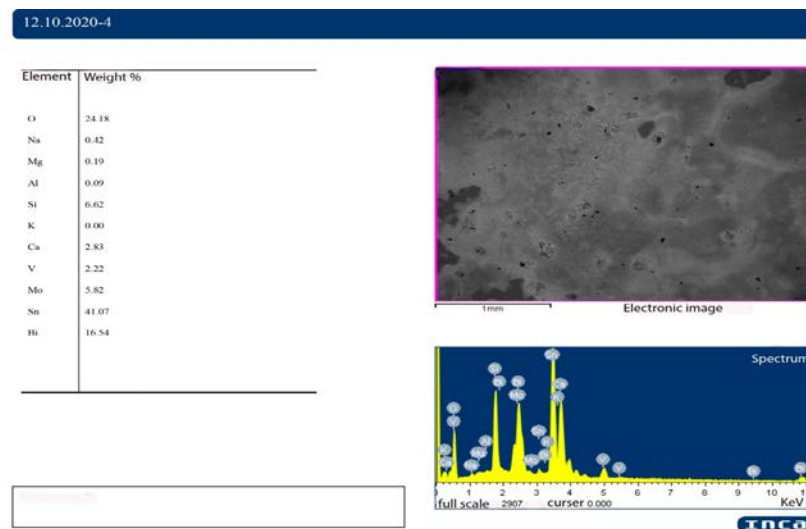


Fig 2. Spectrogram and micrograph of bismuth vanadate film

Fig. 3 shows micrographs of obtained coatings and their morphological properties. It can be seen that the doped bismuth vanadate coating is denser and more compact (1), while the coating without molybdenum appears to be looser in composition and porous (2). The coatings are shown after the application of 10 aerosol layers. With 30 layers of aerosol coating, the coating naturally has a continuous and more uniform surface. These films are shown in the upper corner sections of the photographs.

Nevertheless, here changes in morphology are also noticeable - there is a noticeable porosity of the vanadate layer (2). We will continue our research related to improving the surface - uniformity and continuity, in order to further relate them to the current characteristics of coatings.

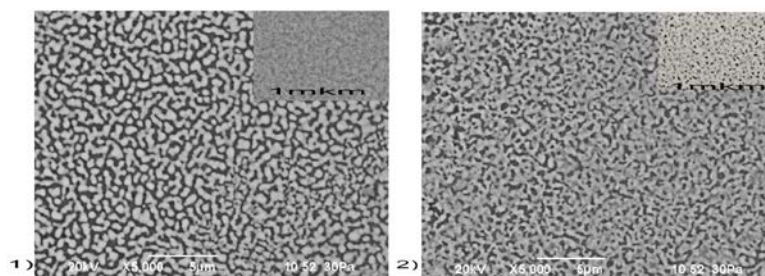


Fig 3. Micrographs and morphological properties of coatings of bismuth vanadate (1) and bismuth vanadate with molybdenum in the film composition (2)

Fig. 4 shows photocurrents of bismuth vanadate films doped with molybdenum. It can be seen that addition of molybdenum dopant increases the current characteristics of glasses by almost an order of magnitude, especially at 0.2% ammonium molybdate content.

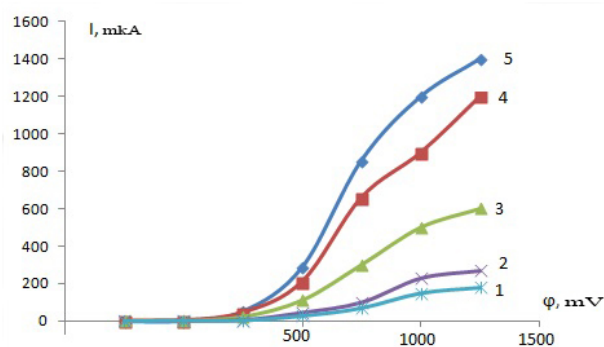


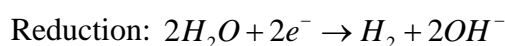
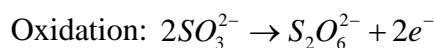
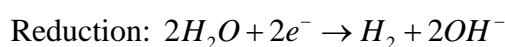
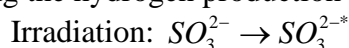
Fig 4. Current-voltage characteristics of films doped with molybdenum: initial bismuth vanadate without Mo (1), at  $(\text{NH}_4)_2\text{MoO}_4$  content 0.1% (2), 0.8 (3), 0.4% (4), 0.2% (5)

Obviously, 0.2-0.4% is the optimal content of molybdenum alloying addition in the mixture used for research, while in other cases this effect is not so obvious. The effect of molybdate ions is often explained in terms of two concepts of catalysis processes: on the one hand, it is associated with decrease of the concentration of states of electron traps, which causes an increase in the mobility of electrons and holes, or with an increased concentration of charge carriers caused by electron-donor elements, in particular, molybdenum. It was also reported [28, 29] about change in the band gap and movement of the band edges, as in our case with additional absorption in the absorption spectra in Figure 1. We call this concept as "current". On the other hand, there is another concept of improving the properties of bismuth vanadate with molybdenum, which is associated with increased adsorption capacity of the photocatalyst due to its higher surface acidity [23]; we call it the "catalytic" concept.

These previous studies of  $\text{BiVO}_4\text{-Mo}$  are based on the hypothesis that Mo (VI) replaces V (V) in the monoclinic main lattice of  $\text{BiVO}_4$  of the scheelite type [23]; i.e. the inclusion of Mo in  $\text{BiVO}_4$  leads to stabilization of the tetragonal scheelite type in solid solutions in the entire range of compositions  $\text{Bi}_{1-x}/3\text{V}_{-x}\text{Mo}_x\text{O}_4$  until a sharp structural change in the final term  $\text{Bi}_2(\text{MoO}_4)_3$  occurs [25, 26]. This expanded solubility of molybdenum in tetragonal  $\text{BiVO}_4$  matrices has been widely confirmed in subsequent studies of  $\text{Bi}_{1-x}/3\text{V}_{1-x}\text{Mo}_x\text{O}_4$  compounds as catalysts for the oxidation of organic substrates [27] or candidates for solid electrolytes.

In any case, the processes of doping bismuth vanadate with molybdenum require a more systematic study and focus on the relationships of synthesis, structure, and activity among  $\text{BiVO}_4\text{:Mo}$  solid solutions in order to elucidate the effect of V/Mo substitution on the phase, particle shape, surface area, thermal stability, and catalytic properties of products.

Sacrificial agents or electron donors / hole absorbers play a significant role in the photocatalytic hydrogen production, since splitting of water is an energetically upward reaction ( $\Delta H_0=286$  kJ/mole). Photochemical reactions of sacrificial agents (methanol, ethanol, isopropanol, ethylene glycol, glycerin, glucose, lactic acid, triethanolamine, sodium sulfide, sodium sulfite and sodium sulfide / sodium sulfate) and their decomposition products during the hydrogen production process are presented as follows in the case of sodium sulfite:



Current-voltage characteristics of films doped with molybdenum in a phosphate buffer electrolyte with sodium sulfite addition are shown in Fig. 5. It can be seen that values of the current characteristics increase significantly in the presence of sulfite, more than twofold, i.e. in the "sacrificial" electrolyte, as it should be according to the theory.

Some imbalance occurs in the Mott-Schottky plots of the same electrodes (Figure 6). A graph for the sample with molybdenum addition is straightforward, and its extrapolation to the potential axis gives the values of flat zones potential for the doped electrode about -600 mV (on the scale of potentials relative to the silver chloride electrode).

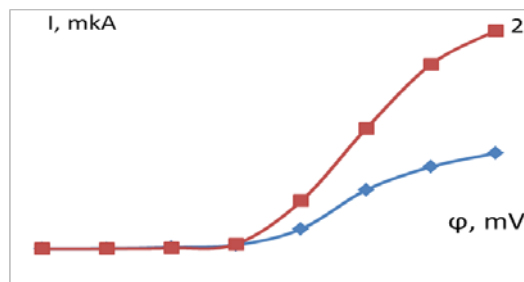


Fig 5. Current-voltage characteristics of films doped with molybdenum in a phosphate buffered electrolyte (1) and in an electrolyte in the presence of sodium sulfite (2)

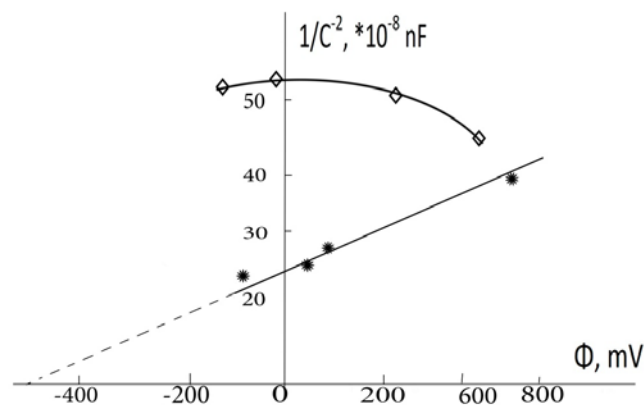


Fig 6. Plots of Mott-Schottky in a sacrificial electrolyte at a frequency of 1 kHz in the investigated potential range

A significant distortion is observed for a sample of pure bismuth vanadate; the data runs in an "arc" and it is difficult to diagnose the flat band potential for a semiconductor. At the same time, for a straight-line graph, the linearity of the Mott-Schottky graph is ideally diagnosed and the potential of flat zones is about -450 millivolts. We associate this with the fact that there is a certain excess of charges at the electrolyte / glass interface in the sacrificial electrolyte. It causes some difficulty in the charge drainage from the surface of electrodes. In the case of doping bismuth vanadate, the semiconductor structure at the interface with the electrolyte appears to be more ordered, and the charges flow faster.

## CONCLUSION

As a result of this study, the current-voltage characteristics of films on the surface of conducting glasses were obtained based on bismuth vanadate doped with molybdenum by the aerosol method from aqueous solutions. Introduction of molybdenum into the bismuth vanadate composition slightly expands the spectral sensitivity of the electrodes in the range of 350 - 470 nm, while the values of the current-voltage characteristics increase almost three times in the phosphate electrolyte. The concentration optimum was found – 0.2% of ammonium molybdate in bismuth vanadate solution, at which photocurrents of the doped electrodes are maximum at aerosol deposition method. It has been established that doping with molybdenum improves the photoelectrochemical properties of photoelectrodes; therefore, it is necessary to continue research to improve the aerosol method of coating deposition as a compact and cheap method for obtaining systems for water photolysis.

## REFERENCES

- 1 Pihosh Y., Turkevych I., Mawatari K., Uemura J., Kazoe Y., Kosar S., Kitamori T. Photocatalytic generation of hydrogen by core-shell  $\text{WO}_3/\text{BiVO}_4$  nanorods with ultimate water splitting efficiency. *Scientific Reports*, 2015, Vol. 5, p.11141. [https://doi:10.1038/srep11141](https://doi.org/10.1038/srep11141).
- 2 Zhang L., Reisner E., Baumberg J.J. Al-doped ZnO inverse opal networks as efficient electron collectors in  $\text{BiVO}_4$  photoanodes for solar water oxidation. *Energy & Environmental Science*, 2014, Vol. 7, pp. 1402-1408. <https://doi.org/10.1039/C3EE44031A>.
- 3 Nair V., Perkins C.L., Linc Q., Law M. Textured nanoporous  $\text{Mo:BiVO}_4$  photoanodes with high charge transport and charge transfer quantum efficiencies for oxygen evolution. *Energy & Environmental Science*, 2016, vol. 9, pp. 1412–1429. <https://doi.org/10.1039/C6EE00129G>
- 4 Hernández S., Gerardi G., Bejtka K., Fina A., Russo N. Evaluation of the charge transfer kinetics of spin-coated  $\text{BiVO}_4$  thin films for sun-driven water photoelectrolysis. *Applied Catalysis B: Environmental*, 2016, Vol.190, pp. 66-74. <https://doi.org/10.1016/j.apcatb.2016.02.059>
- 5 Zhou M., Bao J., Bi W., Zeng Y., Zhu R., Tao M., Xie Y. Efficient Water Splitting via a Heteroepitaxial  $\text{BiVO}_4$  Photoelectrode Decorated with Co-Pi Catalysts. *ChemSusChem*, 2012, Vol. 5, No. 8, pp. 1420–1425. <https://doi.org/10.1002/cssc.201200287>.
- 6 Park Y., McDonald K.J., Choi K.S. Progress in bismuth vanadate photoanodes for use in solar water oxidation. *Chem. Soc. Rev.*, 2013, Vol. 42, pp. 2321–2337. <https://doi.org/10.1039/C2CS35260E>.
- 7 Sivula K. Metal oxide photoelectrodes for solar fuel production, surface traps, and catalysis. *J. Phys. Chem. Lett.*, 2013, vol. 4, pp.1624–1633. <https://doi.org/10.1021/jz4002983>.
- 8 Huang Z.F., Pan L., Zou J.J., Zhang X, Wang L. Nanostructured bismuth vanadate-based materials for solar energy-driven water oxidation: a review on recent progress. *Nanoscale*, 2014, Vol.6, pp. 14044–14063. <https://doi.org/10.1039/C4NR05245E>.
- 9 Kim J. H., Lee J. S.  $\text{BiVO}_4$ -based heterostructured photocatalysts for solar water splitting: a review, *Energy Environ. Focus*. 2014, Vol. 3, pp. 339–353. [https://doi:10.1166/eef.2014.1121](https://doi.org/10.1166/eef.2014.1121).
- 10 Milbrat A., Vijselaar W., Guo Y., Mei B., Huskens J., Mul G. Integration of Molybdenum-Doped, Hydrogen-Annealed  $\text{BiVO}_4$  with Silicon Microwires for

Photoelectrochemical Applications, ACS Sustainable Chemistry & Engineering. 2019, Vol. 7(5), pp. 5034–5044. Doi: [10.1021/acssuschemeng.8b05756](https://doi.org/10.1021/acssuschemeng.8b05756).

11 Kim T.W., Ping Y., Galli G. A., Choi K.S. Simultaneous enhancements in photon absorption and charge transport in bismuth vanadate photoanodes for solar water splitting. Nat. Commun., 2015, Vol. 6, p. 8769. DOI:[10.1038/ncomms9769](https://doi.org/10.1038/ncomms9769)

12 Seitmagzimov A.A., Seitmagzimova G.M. Modification of titanium oxide films by ferric ions in hydrothermal conditions and their photo-electrochemical properties. Asian Journal of Chemistry, 2015, Vol. 27, No. 4, pp. 1521–1524.

13 Walsh A, Yan Y, [Muhammad N. H.](#), Mowafak M. Al-Jassim, Wei Su-Huai. Band edge electronic structure of BiVO<sub>4</sub>: Elucidating the role of the Bi s and V d orbitals. Chem. Mater., 2009, Vol. 21, pp. 547–551. <https://doi.org/10.1021/cm802894z>

14 Cooper J.K, Gul S., Toma F.M., Chen L, Glans P.-A., Guo J., Ager J. W., Yano J., Sharp I. D. Electronic structure of monoclinic BiVO<sub>4</sub>. Chem. Mater., 2014, Vol. 26, pp. 5365–5373. <https://doi.org/10.1021/cm5025074>.

15 Jiang C., Wang R., Parkinson B. A. Combinatorial approach to improve photoelectrodes based on BiVO<sub>4</sub>. ACS Comb. Sci., 2013, Vol. 15, pp. 639–645. <https://doi.org/10.1021/co300119q>.

16 [Zhong D.K.](#), [Choi S.](#), [Gamelin D.R.](#) Near-Complete Suppression of Surface Recombination in Solar Photoelectrolysis by “Co-Pi” Catalyst-Modified W:BiVO<sub>4</sub>. J. Am. Chem. Soc., 2011, Vol. 133, pp. 18370–18377. <https://doi.org/10.1021/ja207348x>

17 Abdi F.F, Savenije T.J., May M.M., Dam B., R. van de Krol. The origin of slow carrier transport in BiVO<sub>4</sub> thin film photoanodes: A time-resolved microwave conductivity study. J. Phys. Chem. Lett., 2013, Vol. 4, pp. 2752–2757. <https://doi.org/10.1021/jz4013257>.

18 Pala R.A., Leenheer A.L., Lichterman M., Atwater H.A., Lewis N.S. Measurement of minority-carrier diffusion lengths using wedge-shaped semiconductor photoelectrodes. Energy Environ. Sci., 2014, Vol. 7, pp. 3424–3430.

19 Rettie A.J. E., Lee H. C., Marshall L. G., Lin J.-F, Capan C., Lindemuth J., McCloy J. S., Zhou J., Bard A. J., Mullins C. B. Combined charge carrier transport and photoelectrochemical characterization of BiVO<sub>4</sub> single crystals: intrinsic behavior of a complex metal oxide. J. Am. Chem. Soc., 2013, Vol. 135, pp. 11389–11396. <https://doi.org/10.1021/ja405550k>.

20 Pilli S. K., Furtak T. E., Brown L.D., Deutsch T.G, Turner J.A., Herring A. M. Cobalt-phosphate (Co-Pi) catalyst modified Mo-doped BiVO<sub>4</sub> photoelectrodes for solar water oxidation. Energy Environ. Sci., 2011, Vol. 4, pp. 5028–5034. <https://doi.org/10.1039/C1EE02444B>.

21 Cooper J.K, Gul S., Toma F. M., Chen L., Glans P.A., Guo J., Ager J. W., Yano J., Sharp I. D.. Electronic structure of monoclinic BiVO<sub>4</sub>. Chem. Mater., 2014, Vol. 26, pp. 5365–5373. <https://doi.org/10.1021/cm5025074>

22 McDowell M.T., Lichterman M.F., Spurgeon J.M., Hu S., Sharp I.D., Brunshwig B.S., Lewis N.S. Improved stability of polycrystalline bismuth vanadate photoanodes by use of dual-layer thin TiO<sub>2</sub>/Ni coatings. J. Phys. Chem. C, 2014, Vol. 118, pp. 19618–19624. <https://doi.org/10.1021/jp506133y>.

23 Jin J., Walczak K., Singh M. R, Karp C., Lewis N. S., Xiang C. An experimental and modeling/simulation-based evaluation of the efficiency and operational performance characteristics of an integrated, membrane-free, neutral pH solar-driven water-splitting system. Energy Environ. Sci., 2014, Vol. 7, pp. 3371–3380. <https://doi.org/10.1039/C4EE01824A>.

- 24 Kontic R., Patzke G. Synthetic trends for BiVO<sub>4</sub> photocatalysts: Molybdenum substitution vs. TiO<sub>2</sub> and SnO<sub>2</sub> heterojunctions. *Journal of Solid State Chemistry*, 2012, Vol. 189, pp.38-48. Doi: [10.1016/j.jssc.2011.11.050](https://doi.org/10.1016/j.jssc.2011.11.050).
- 25 Luo W., Li Z., Yu T., Zou Z. Effects of surface electrochemical pretreatment on the photoelectrochemical performance of Mo-doped BiVO<sub>4</sub>, *J. Phys. Chem. C*, 2012, Vol. 116, pp. 5076–5081. <https://doi.org/10.1021/jp210207q>.
- 26 Karolina Ordon. Functionalized semiconducting oxides based on bismuth vanadate with anchored organic dye molecules for photoactive applications. *Physics [physics]*. Université du Maine, 2018. <https://tel.archives-ouvertes.fr/tel-01849209>.
- 27 Sivakumar V., Suresh R., Giribabu K., Narayanan V. BiVO<sub>4</sub> nanoparticles: Preparation, characterization and photocatalytic activity. *Cogent Chemistry*, 2015, Vol. 1, p. 1074647. <http://dx.doi.org/10.1080/23312009.2015.107464>.
- 28 Luo W., Yang Z.,<sup>a</sup> Li Z., Zhang J., Liu J., Zhao Z., Wang Z., Yan S., Yu T., Zou Z. Solar hydrogen generation from seawater with a modified BiVO<sub>4</sub> photoanode. *Energy Environ. Sci.*, 2011, Vol. 4, pp. 4046-4051. <https://doi.org/10.1039/C1EE01812D>.
- 29 Pattengale B., Huang J. The Effect of Mo Doping on The Charge Separation Dynamics and Photocurrent Performance of BiVO<sub>4</sub> Photoanodes. *Physical Chemistry Chemical Physics*, 2016, Vol. 18, No. 48, pp. 32820-32825.
- 30 Nair V., Perkins C.L., Linc Q., Law M. Textured nanoporous Mo:BiVO<sub>4</sub> photoanodes with high charge transport and charge transfer quantum efficiencies for oxygen evolution. *Energy Environ. Sci.*, 2016, Vol. 9, pp. 1412-1429, Doi: 10.1039/c6ee00129g.